MAR 1 : 1986

CONF-860102--16

Recent BeO-Reflect[illegible] d Reactor Experiments in Z[illegible]PR

H. F. [illegible], S. [illegible]h, S. G. Carpenter
[illegible] [illegible] Knight

Arg[illegible] National Laboratory
P.O. Box 2528
Idaho [illegible] ID 83[illegible]-2528

CONF-860102--16

DE86 007517

DISCLAIMER

Work supported by the U.S. [illegible] [illegible] Nuclear Energy Programs under Contract W-31-109-Eng-38.

MASTER

Recent BeO-Reflector-Controlled Reactor Experiments in ZPPR

Harold F. McFarlane, Stephen B. Brumbach, Stuart G. Carpenter,
Peter J. Collins and Richard D. McKnight
Argonne National Laboratory
P.O. Box 2528
Idaho Falls, ID 83403-2528

ABSTRACT

Integral reactor physics measurements were performed on a BeO-reflected fast reactor assembly in the ZPPR facility during January and February of 1985. The measurements emphasized power distributions and reflector control worths in two different critical states. The measurements have been analyzed using three-dimensional deterministic and Monte Carlo methods and the ENDF/B-V.2 nuclear data library. Together the measurements and analyses form a modern, reliable, benchmark data set for testing calculational methods that will be used in predicting some of the design parameters for future space reactors.

INTRODUCTION

Benchmark reactor physics experiments were conducted on a BeO-reflected, uranium-oxide-fuelled fast reactor assembly in the Zero Power Plutonium Facility (ZPPR) during January and February of 1985. These experiments, known as the ZPPR-14 Program, provide integral physics data on a reactor system with physics characteristics typical of some reactors recently proposed for space power applications. The measurements have been analyzed using the most powerful techniques presently available to fast reactor physicists. The recency of these experiments is significant in that measurement capabilities have evolved substantially in the intervening years since any previous relevant experiments were done. Only a few earlier experiments addressed the combination of a beryllium reflector and a fast reactor core (Stewart et al. 1958, Butler et al. 1966, and Callen et al. 1965).

The ZPPR facility (Lawroski et al. 1972), located at the Idaho National Engineering Laboratory (INEL) in eastern Idaho, is operated by the Applied Physics Division of Argonne National Laboratory (ANL). ZPPR has been used principally in the Department of Energy's (DOE) liquid metal fast breeder reactor (LMFBR) development program. After a loading period of several weeks, fast-neutron-spectrum reactors in ZPPR have their physics characteristics determined through a series of measurements that may

include criticality, power distributions, control system worths, reactivity coefficients, reaction rate ratios, shielding effectiveness, neutron and gamma fluences, spectra and breeding, among others. Generally, the reactors are built by loading "plates" of discrete materials into a ZPPR subassembly called a "drawer," and then arranging the drawers in a large stainless steel matrix. The facility is quite flexible, accommodating other loading arrangements, reactors of all sizes, and substantial variation in composition.

Part of the ZPPR matrix is shown in Figure 1 with one of the ZPPR-14 configurations loaded. Since ZPPR is of the split-table design, the very center of the reactor core is visible in the photograph. The ZPPR-14 assembly was based on a conceptual design for a small terrestrial liquid metal fast reactor. The design borrowed several features, including the reflector control concept, from the Systems Auxiliary Nuclear Power (SNAP) space reactor program of the 1960's and 1970's. In the ZPPR-14 Program, the BeO reflector was divided into four segments which were moved axially and radially. In Figure 1, the reflector segments have been moved radially out away from the core in a simulated secondary scram condition. The photograph was taken during one step in a series of measurements to determine the reflector worth characteristics of the system.

The ZPPR-14 Program was quite brief. The intent was to obtain benchmark data for just the basic core parameters -- critical loading, power distribution and control worth. There simply was not time to measure other key parameters such as reactivity coefficients.

The SP-100 Program provides the immediate focus for space nuclear power. Comparisons between some reactor physics properties of a "typical" SP-100 design and ZPPR-14 are presented in Table 1 and Figure 2. The SP-100 data have been calculated for a 100 kWe reactor which is substantially smaller than ZPPR-14. However, with the increase in size of SP-100 from 100 kWe to 300 kWe, the SP-100 parameters should move closer to the ZPPR-14 values.

Considering first the neutron balance comparison in Table 1, the key item is the comparison of the radial leakage terms, which substantially govern the reflector control properties of each system. For consistent designs, the SP-100 will have less radial leakage in the 300 kWe size, making the comparison with ZPPR-14 reasonably favorable. The fission terms agree because they are both ^{235}U systems that have been normalized by the fission source. Capture in ZPPR-14 is substantially greater because the ^{238}U fraction is more than an order of magnitude greater. There is a large

difference in axial leakage because the length to diameter ratio of ZPPR-14 is about 2.5 times that of SP-100. Axially varying parameters in ZPPR-14 are thus not very representative of proposed SP-100 designs.

The neutron spectra comparison in Figure 2 shows the SP-100 spectrum to be notably harder than that in the ZPPR-14 spectrum, as would be expected because of the factor of three difference in average enrichment. The spectral difference is most apparent in differences between the two cores with respect to ^{238}U fission and capture rates, neither of which are very important in the fully enriched SP-100 core. A larger SP-100 core probably would have a substantially higher ^{238}U fraction, hence more inelastic scattering and a softer spectrum, closer to that of ZPPR-14. Since the SP-100 was modeled with nitride fuel, its spectrum does not exhibit the large oxygen resonance that is apparent in the ZPPR-14 spectrum. The flat adjoint spectrum shown for ZPPR-14 is typical for a ^{235}U-fuelled fast reactor.

Analyses of the ZPPR-14 measurements utilized advanced methods most likely to be of interest to designers. All calculations were done using cross sections derived from the Evaluated Nuclear Data Files (ENDF/B) Version V, Revision 2. Because of the effort and expense involved, some measurements have not yet been analysed, and some have been calculated only with the simpler analysis models.

PROGRAM DESCRIPTION

Reactor Description

The ZPPR-14 assemblies constructed for the benchmark experiments consisted of two critical and numerous subcritical configurations representative of a low-power density, 40-MWt, sodium-cooled fast reactor. A cross-sectional view of ZPPR-14 is shown in Figure 3. The reactor core was constructed from unit cells (subassemblies) of the type shown in Figure 4. The 93%-enriched ^{235}U plates are combined in proper proportion with the depleted U_3O_8 plates to give the correct average enrichment for the critical core loading. With the other materials in the cell, the average composition is close to that of a UO_2 subassembly in a sodium-cooled fast reactor. The heterogeneity effect of using plates rather than pins is on the order of one percent of the critical eigenvalue. When inserted in the matrix, the typical dimension of one of the cells is about 55 mm. With 12 such cells to span the core, the diameter was about 660 mm. The core had an overall height of almost 1.8 m.

The downcomer region, representing both the sodium downcomer and the core barrel, was only one cell thick. It was comprised of sodium, stainless steel and void.

The reflector region had an average thickness of 205 mm, composed principally of BeO in stainless steel drawers and matrix. However, in the first critical configuration (ZPPR-14A), which simulated an end of cycle condition with the reflector inserted over the full core height, there was insufficient inventory to build the reflector entirely from BeO. Therefore, BeO was used in the two rings of cells closest to the core, Be metal was mostly used in the third ring, and graphite was mostly used in the fourth ring. In the ZPPR-14B configurations, representing a mid-cycle state with the reflector half inserted, only BeO was used to construct the entire reflector.

Outside the reflector was a large void region consisting of empty ZPPR matrix tubes. This region extended about 560 mm beyond the reflector.

Terminating the void was a massive, three-region, radial shield. The inner cell of the shield consisted of B_4C, sodium and stainless steel. The next layer of the shield was graphite, followed by over 150 mm of stainless steel.

There was also extensive axial shielding of the ZPPR-14 assemblies. Each end of the reflector and void regions was shielded by 150 mm of depleted uranium, followed by 310 mm of graphite and another 150 mm of stainless steel. At either end of the core, there was a sodium and stainless steel plenum region extending for 432 mm. These plena were capped with 150 mm of solid stainless steel, which extended out to the inner edge of the radial shield region. The downcomer extended over the full axial height between the two stainless steel planes.

There were two reference configurations for the ZPPR-14 Program. In the ZPPR-14A reference loading, the reflector surrounded the downcomer over the full core height. The effective enrichment was 30%, with a ^{235}U loading of about 500 kg. There were also 40 kg of plutonium (27% ^{240}Pu) in the core to provide a distributed neutron source for the subcritical configurations. In the second critical reference configuration, the BeO reflector covered only half the core height. Void remained in place of the part of the reflector that was removed. A schematic of the ZPPR-14B core configuration is shown in Figure 5. In this configuration the effective enrichment was increased to about 34% to maintain system criticality. Core-average

enrichment in ZPPR-14 was adjusted by varying the ratio of the two core cell types shown in Figure 4.

Measurements

Although the measurement program was brief, a fairly extensive data base was acquired. Of course, the critical loading conditions for the two reference configurations were determined. Measurements of reflector control worth were emphasized, since that represented the area of principal design concern. Detailed spatial maps of many key reaction rates were also obtained, and ^{235}U fuel worth was measured as a function of radius.

Reflector Control Worths

For the control worth measurements, the reflector was assumed to be built in independently movable segments. The segments were assumed to be able to move axially and to be able to pop radially out away from the core barrel, roughly 250 mm outboard from their reference positions. The latter is the designated secondary scram mode. Figure 6 shows the types of altered reflector configurations that were allowed.

In the configuration on the left side of Figure 6, neutron streaming gaps of about 110 mm have been created at four symmetrical locations along the full height of the core. This was done in part to model structural gaps that would be present with operational reflector segments. (The 424 ZPPR drawers comprising the reflector had to be moved individually for changes in reflector configuration.) However, it was also felt that this case might also prove to be a useful diagnostic example for analysis of the secondary scram configurations.

In the configuration in the center of Figure 6, one of the reflector segments has been completely removed. This simulates full axial withdrawal of the reflector segment, the primary scram mode. Measurements were made with one, three and all four segments removed in this manner. In ZPPR-14A, the worth of putting the reflectors in the ZPPR-14B reference state was also measured.

In the configuration on the right side of Figure 6, one of the segments has been moved out into the secondary scram position. Measurements of this type were only made relative to the ZPPR-14B reference configuration. One, three and all four segments were moved in this manner.

The reflector worth measurements were made using the modified source multiplication technique (Carpenter 1976) that has been substantially

refined over the years at ZPPR. Sixty-four ^{235}U fission chambers were distributed throughout the assembly to obtain the data needed for the worth measurements. The fission chambers are built into 150-mm-long stainless steel cans that normally contain sodium, so that they fit into a normal unit cell with a minimum of perturbation. Although the data from the chambers were taken in order to measure the reflector worths, they also provide a coarse power distribution map for a number of configurations.

In measuring the change in system reactivity, it is necessary to know approximately how the relative power distribution changes between the perturbed and the reference states. This is a principal reason for using such a large number of in-core chambers in ZPPR. Figure 7 shows the relative change in ^{235}U fission distribution when one of the reflector segments was removed from ZPPR-14. There is a 5% change between the contours in the figure, starting at 1.15 and going down to 0.30. The values for the contour lines are the ratio of two ratios. The first is the ratio of the fission rate at a point to the total fission integral in the perturbed system. The second is the same type ratio, but in the unperturbed reference system. It is evident from Figure 7 that there are large relative power redistributions associated with the reflector movement. For example, the changes observed in the ZPPR-14 measurements are considerably larger than is observed for B_4C control rod measurements in LMFBR assemblies. Such large flux redistributions not only make analysis of the measurements difficult, but they make it essential to have spatially distributed instrumentation in order to achieve reasonable accuracy in the measurements themselves.

Reaction Rates

Reaction-rate distributions in both reference critical configurations of ZPPR-14 were measured for ^{235}U fission, ^{239}Pu fission, ^{238}U capture and fission, and gamma-ray heating. The neutron reaction rates were measured using thin foils of about 250 mg mass distributed throughout the reactor by slipping them in between plates of normal material (Brumbach et al. 1982 and 1985). The gamma heating rates were measured in stainless steel with thermoluminescent dosimeters (TLDs).

^{235}U fission rates were measured throughout the ZPPR-14 assembly. Data are available for 185 positions in ZPPR-14A and 174 positions in ZPPR-14B. There were detailed radial, axial and azimuthal core maps. Measurements were also made in the downcomer, the reflector, the void zone, the radial shield and the axial plena. The data outside the core zone provide a partial test for ex-core shielding calculations.

Measurements of ^{238}U and ^{239}Pu reaction rates were restricted to the core region. ^{238}U measurements were made at 72 locations in ZPPR-14A and 42 locations in ZPPR-14B. ^{239}Pu measurements were made at 24 locations in ZPPR-14A and 29 in ZPPR-14B.

Gamma-ray dose rates were measured with ^{7}LiF and CaF_2 TLDs. The TLDs are 1 mm square by 6 mm long. They fit snugly in a 6.4 mm by 12.7 mm stainless steel cylinder, which is placed inside a special sodium plate in the core cells. Outside the core, in downcomer and plenum regions that contain sodium plates, the TLDs were contained in 12.7 mm by 3 mm stainless steel cylinders which were placed in the small air cooling gap between cells. Radial measurements extended out beyond the radial shield. The gamma heating map of the ZPPR-14A assembly included182 TLDs, while 196 TLDs were used in the ZPPR-14B assembly.

Analysis Methods

The ZPPR-14 analysis has bee done by diffusion theory, transport theory and Monte Carlo calculations. Cross section data for both the deterministic and the Monte Carlo calculations were derived from the latest nuclear data library release, ENDF/B-V.2. In all cases, only three-dimensional geometrical modeling was used. Thirty energy groups were used for all the deterministic calculations.

Multigroup Cross Section Preparation

The ETOE-2/MC^2-2/SDX (Toppel et al. 1978) code package was used to process the ENDF/B basic nuclear data into a 30-group cross section set. The ETOE-2 code takes the basic nuclear data for all the relevant isotopes from the ENDF/B files and prepares files that can be used directly by MC^2-2 and SDX. MC^2-2 is a dimensionless slowing-down code that is used to calculate an ultra-fine group spectrum. SDX is a one-dimensional code that is used to collapse (in space and energy) the fine group isotopic data to the homogenized multigroup cross sections.

MC^2-2 was used to calculate a 2082-group spectrum for the homogeneous composition of the ZPPR-14 double-fuel-column cell with a buckling search to critical. Thermal group cross sections, not normally available in this fast-spectrum calculational path, were added to the MC^2-2 files at the ultra-fine group level. Cross sections for such materials as plutonium that were in the reactor assembly, but not in the reference core cell, were added at infinite dilution. The isotopic cross section data were collapsed to 226 groups using the MC^2-2 calculated spectrum.

Cell calculations at the 226 (fine-group) level were made in the SDX code for the fuel cells using a buckling search to critical, and for the depleted uranium part of the axial shield using zero buckling. Group collapse to form a 30-group library was done using the asymptotic cell spectrum calculation as one of two approaches. The other approach used a one-dimensional reactor model to calculate the 226-group spectrum in different regions, with the group collapse being done within defined regions. Data from the latter approach were used for reference calculations in the ZPPR-14 Program. One model represented the core, downcomer and reflector A second model represented the core, downcomer and void (typical of the top half of ZPPR-14B). A third model represented the core and the sodium-filled region above the core. In each model, the data for the outer region of the core (~50 mm) were collapsed separately from those in the interior. This was done simply in recognition of the very rapid spectrum transition between the core and the beryllium reflector. The 30-group structure also represented a concession to the lower-energy neutrons returning from the reflector. The last group of the standard 28-group ZPPR structure was subdivided into three groups including a thermal group.

An RZ model of ZPPR-14 was used to test the sensitivity of the calculations to the different group collapse schemes. Nine calculations were run with varying combinations of asymptotic and spatially collapsed cross section data. The difference in calculated k_{eff} for the system between using all asymptotic cross sections and all spatially collapsed cross sections was 4.9%. The effect was made up principally from the radial reflector cross sections (3.7%) and the downcomer cross sections (1.2%). The effect of switching core data sets was less than 0.1%. The high sensitivity to cross sections in the regions where the spectrum is softer gives rise to some concern about the adequacy of the thermal group data that were added to the the MC^2-2 files, since they were not generated specifically for this reactor.

Deterministic Calculations

All deterministic calculations for ZPPR-14 were made with the DIF3D code (Derstine 1982 and Lawrence 1983) using Cartesian geometry and 30 energy groups. In this geometry, the code has options for finite-difference diffusion theory calculations, nodal diffusion theory calculations, and nodal transport theory calculations. Each of these options was used in part of the ZPPR-14 analysis. A mesh spacing of 55 mm, corresponding to unit cell dimensions, was used in the XY plane. The axial mesh spacing was about 51 mm over most of the core height.

The finite-difference diffusion calculations were used in a truncated model that included only part of the empty matrix beyond the radial reflector, but retained the full axial dimension of the system. The X and Y boundary conditions were chosen so as to reduce the effect of the truncation on the core fission distribution with the reflectors removed. (The effect was trivial with the reflectors in place.) The truncated model was used for a number of reasons. First, calculations with quick turn-around time were required for use in reducing data from the measurements (basically for interpolating fission distributions between measured points). The truncated model had only one-quarter of the XY-mesh storage requirement of the full radial model. Since many of the perturbed reflector configurations were not symmetric in the XY plane, the compromise was necessary in order to get the necessary calculations done. Second, since this model was only used for diffusion calculations, including that part of the assembly beyond the reflector was not felt to be sufficiently meaningful to justify the extra expense.

The nodal calculations have only been used for measurements that preserved symmetry in the XY plane. The models used were:

- one-quarter XY, half Z for ZPPR-14A
- one-quarter XY, full Z for ZPPR-14B.

The full radial extent of the assembly, out through the last stainless-steel shield zone, was included in each of these models.

The nodal transport calculational method used here is an approximate method in a developmental version of the DIF3D code, and is available only for Cartesian geometry (Lawrence 1984). It has been tested in LMFBR systems built in ZPPR and shown to compare favorably with low-order S_n solutions.

Monte Carlo Calculations

The Monte Carlo solutions have been computed with the VIM code (Blomquist 1980). VIM is capable of explicit three-dimensional modeling all spatial details of the assembly. It is a continuous-energy code, so that there are no multigroup approximations. Also, special BeO nuclear data, including thermal upscatter, were used in the VIM calculations.

VIM was used to calculate the two reference configurations and three of the symmetric perturbed reflector configurations. The VIM models were slightly idealized in that some details of the experiment were omitted for

simplicity (detectors, operational shim rods at the axial edges of the core, minor temperature differences). Small corrections (0.0005-0.0035 Δk) for the effects of these approximations were made using deterministic results. Two-hundred thousand neutron histories were run for the reference cases and 100,000 for the perturbed cases. With this many histories, the eigenvalue statistics are about 0.002 for one standard deviation.

RESULTS

Critical Configurations

The results of eigenvalue analysis for the two reference critical configurations are presented in Table 2. The measured k_{eff} values listed for the two assemblies are for states with the operational shim rods withdrawn to the maximum reactivity positions. The experimental uncertainties are dominated by limits on the ability to describe the composition of the system.

The Monte Carlo results for ZPPR-14 of 0.9962 and 0.9988 for the ratio of the calculated to measured (C/E) values of k_{eff} are consistent within the statistics of the calculations. Values near unity are also consistent with other Monte Carlo calculations for ^{235}U-fuelled fast reactors when using the ENDF/B-V nuclear data library.

The deterministic calculations indicate a notable discrepancy between the ZPPR-14A and ZPPR-14B results, with the transport C/Es differing by 0.9% and the diffusion C/Es differing by 1.2% for the two cases. The evidence suggests that the problem lies in the multigroup cross section processing, most likely for the reflector and downcomer regions.

The 0.8% difference between the diffusion and transport C/Es in the ZPPR-14B case is typical for high-leakage fast reactor systems. It is interesting to note that in the fully reflected case, the transport correction to the diffusion calculation is only about 0.4%. The relative adequacy of diffusion theory calculations in the 14A assembly also shows up in the reaction rate analysis.

Table 3 gives the ^{235}U fuel worth as a function of radius in ZPPR-14A. Although the measurements were done with quarter-core symmetry to facilitate analysis, no calculations of these data are yet available. The measurements were done by removing the ^{235}U from four symmetric double-column cells of the type shown in Figure 4.

Reaction Rates

The ZPPR-14 Program contained too much reaction rate data to be presented in any detail here, so the results have been reduced to summaries of the power distributions and the reaction rate ratios.

Figure 8 shows the radial reaction rate distributions in the fully reflected ZPPR-14A core. The measured data are indicated by markers, while the lines are the results from the nodal transport calculations. The radial distributions are flatter than might have been expected, as some beryllium-reflected designs have shown considerably more power peaking near the core edge. There is some upturn in the ^{239}Pu and ^{235}U fission rates near the boundary, but apparently the downcomer region provides a substantial buffer. The calculated rates match the measured ^{235}U fission distribution well over the interior of the core, but are off by 6% for the two outermost positions. The calculation of ^{239}Pu fission does not track the upturn nearly as well. The reason for the disparity is in the difference in the way the 30-group cross sections were prepared. The plutonium cross sections were collapsed from 226 groups to 30 groups in the asymptotic cell spectrum, whereas the uranium cross sections were collapsed in the one-dimensional reactor calculation with two core regions. Also, there were no thermal data for plutonium available at the time the cross sections were being prepared, and the default thermal-group values that were used were unrealistically low.

The in-core distribution of gamma heating rates in stainless steel are also shown on the same plot in order to compare to the distribution shapes. All the data have been normalized to an average core power of one watt. In Figs. 8-10, the units for the neutron reaction rates are 10^{-17} reactions per atom per second; the units for the gamma heating measurements are 10^{-5} Gy/s. No calculations are available for any of the gamma heating measurements.

The well-behaved power distribution in the core may be contrasted with the radial fission rate plot for the whole assembly, shown in Figure 9. Two radial traverses are shown for ZPPR-14B, one at an axial position such that the traverse went through the reflector, the other starting from a spot higher on the core, so that it went through additional void zone rather than the reflector. Again, the solid lines indicate the results of a transport calculation. The calculation is clearly unable to track the fission rate through the reflector; beyond the reflector the C/Es are on the order of 2.0. Similarly, the calculations overpredict the reaction rates in the unreflected traverse by about 60% at large radius. Part of the problem is the difficulty in computing the self-shielding for the foils used in the measurements beyond the core region.

Figure 10 shows axial power distribution near the central axis in the half-reflected ZPPR-14B core. The shift in power to the reflected half is substantial. Unlike the situation in the fully reflected case, the calculations were unable to track the measurements inside the core. The C/E ratios are about 1.08 in the reflected half and about 0.93 in the unreflected half. The results shown are from the transport calculations, but they offer no substantial improvement over the diffusion theory results. The measured power contribution from gamma heating is shown in the same plot. The principal difference in shape occurs in the plenum region, as would be expected.

Axial power peaking is summarized in Table 4. for both reference configurations. The first entry under ZPPR-14B corresponds to the data plotted in Figure 10. In ZPPR-14A, there was little radial variation in the axial peak/average power ratio. The nominal value of 1.3 was well predicted by the transport calculation. Considerably more radial variation can be observed in the ZPPR-14B axial peak/average factors, but the predictions provided by the transport calculations are reasonably consistent. The overprediction of 3-4% in the 14B case can be correlated with the overprediction of reflector worth by deterministic methods.

The reaction rate ratio results are summarized in Table 5. As might be anticipated from Figure 7, they form a fairly consistent set. Also, since all the data were taken in the core, there are no major discrepancies between the measurements and the transport calculation results. The increase in the fission ratios from ZPPR-14A to ZPPR-14B is evidence of the hardening of the spectrum with the increase in average enrichment. There is a concomitant decrease in the capture-to-fission ratio. The C/E ratios are consistent with others that have been noted for calculations of fast reactor systems with ENDF/B-V.2 nuclear data.

Reflector Control Worths

There were five perturbations to the reference reflector configuration in each of the two reference assemblies. Briefly, the perturbations were chosen to simulate the following conditions:

- Full primary scram mode
- Full secondary scram mode
- Single segment scram in either mode
- Single segment failure to scram in either mode

- 14B configuration relative to 14A reference
- Gaps between reflector segments.

The worths of these perturbations ranged from four dollars to 30 dollars. They are summarized in Table 6, along with the results of the calculations. Only three cases have been analyzed with the calculational methods being tested. The complete column of C/Es on the far right-hand side of Table 6 are from the calculations done with the model that was truncated in the XY plane. Since the boundary condition in this model was chosen to preserve core reaction rates and not eigenvalue, these results were not expected to be meaningful. Nevertheless, they form a surprisingly consistent set with one exception. The exception is the case where the narrow gaps were formed, and is clearly not amenable to diffusion theory modeling.

Although both the nodal diffusion and transport calculations overpredict the reflector worths, the transport solutions clearly form a more consistent set. This is expected since there is a sizable transport correction for the reference ZPPR-14B eigenvalue calculation. The diffusion theory results may look favorable enough to be deemed adequate for some conceptual modeling calculations.

The Monte Carlo calculations slightly underpredict the reflector worths, but form by far the most consistent set of analyses. The degree of underprediction is almost insignificant when considering the 3% statistics on the calculations.

CONCLUSIONS

The ZPPR-14 Program has provided high-quality benchmark data for some of the key reactor physics parameters of a BeO-reflected fast reactor. Analyses of these data can provide useful guidance in the selection of calculational tools to be used in the design of space reactors of this type. The data are not an acceptable substitute for integral physics measurements for a specific design such as SP-100, but they can identify some of the problems that need to be avoided.

The Monte Carlo calculations with ENDF/B-V.2 nuclear data performed well in all aspects of the analysis, even relative to previous test results obtained for more typical fast reactor systems. However, the exclusive use of such calculations in a design program is not practical, since so much effort is required to set up the models and essentially no spatial detail is obtained from the whole-core calculations. The calculations already

completed need to be edited further to check such parameters as the ratio of powers in the reflected and unreflected halves of ZPPR-14B.

Extreme care must be taken in the prepartion of multigroup cross sections to be used in deterministic design analysis for a reactor of this type. Collapse to the final group structure must be done in a calculation that models each specific region in the system as a whole. Despite the precautions taken in this work, many questions remain unanswered relative to errors in the cross sections. The effect of more careful selection of the thermal-group cross sections is unknown. Because of the high sensitivity of the calculations to group collapse in the reflector, it has been suggested that Monte Carlo calculations be used to generate absorption cross sections for the reflector and possibly the downcomer.

The source of concern about multigroup cross sections is that the neutron spectrum changes so substantially over such a short distance between the core and the BeO reflector. This problem will be worse in most space reactor designs, since the reflector will be closer to a more highly enriched core.

ACKNOWLEDGMENTS

This work was done at Argonne National Laboratory, supported by the U. S. Department of Energy, Nuclear Energy Programs, under contract No. W-31-109-Eng-38. The authors also wish to acknowledge their colleagues at the ZPPR facility for their very substantial role in the success of the ZPPR-14 Program. T. Misawa, a student from Japan, helped with the Monte Carlo calculations during his assignment to Argonne.

REFERENCES

H. B. Stewart and M. L. Storm (1958) "The Critical Assembly Program", in *Naval Reactor Physics Handbook*, Vol. III, U. S. Atomic Energy Commission, Washington, D. C.

D. K. Butler, R. C. Derner and W. G. Knapp (1966) "Measurements and Analysis of Al-, Al_2O_3- and BeO-reflected Fast Critical Experiments," in *Proc. of International Conference on Fast Critical Experiments*, Argonne National Laboratory, Argonne, Illinois, 13-16 October, 1966.

R. C. Callen, P. S. Check, R. E. Kearney and W. F. Walsh (1965) *SNAP-50 Critical Experiments and Analysis*, PWAC-487, Pratt and Whitney Aircraft Corporation, Middletown, Connecticut, September 1965.

H. Lawroski, R. G. Palmer, F. W. Thalgott, R. N. Curran and R. G. Matlock (1972), *Final Safety Analysis Report on the Zero Power Plutonium Reactor (ZPPR) Facility*, Argonne National Laboratory, Argonne, Illinois, June 1972.

S. G. Carpenter (1976) "Measurement of Control Rod Worths Using ZPPR" in *Proc. of Specialists Meeting on Control Rod Measurement Techniques: Reactivity Worth and Power Distributions*, NEACRP-U-75, C. E. N. Cadarache, France, 21-22 April 1976.

S. B. Brumbach and J. M. Gasidlo (1985), *In-Cell Reaction Rate Distributions and Cell-Average Reaction Rates in Fast Critical Assemblies*, ANL-85-44, Argonne National Laboratory, Argonne, Illinois.

S. B. Brumbach and D. W. Maddison, Reaction Rate Calibration Techniques at ZPPR for ^{239}Pu Fission, ^{235}U Fission, ^{238}U Fission and ^{238}U Capture, ANL-82-38, Argonne National Laboratory, Argonne, Illinois.

B. J. Toppel, H. Henryson II and C. G. Stenberg (1978) "ETOE-II/MC^2-2/SDX Multigroup Cross Section Processing," in *Proc. of RSIC Seminar Workshop on Multigroup Cross Sections*, Oak Ridge National Laboratory, 14 March 1978.

K. L. Derstine (1982) *DIF3D: A Code to Solve One-, Two-, and Three-Dimensional Finite-Difference Diffusion Theory Problems*, ANL-82-64, Argonne National Laboratory, Argonne, Illinois.

R. D. Lawrence (1983) The DIF3D Nodal Neutronics Option for Two- and Three-Dimensional Diffusion Theory Calculations in Hexagonal Geometry, ANL-83-1, Argonne National Laboratory, Argonne, Illinois.

R. D. Lawrence (1984) "Three-Dimensional Nodal Diffusion and Transport Methods for the Analysis of Fast-Reactor Critical Experiments," in *Trans. of Topical Meeting on Reactor Physics and Shielding*, Chicago, Illinois, 17-19 September 1984.

R. N. Blomquist, R. M. Lell and E. M. Gelbard (1980) "VIM -- A Continuous Energy Monte Carlo Code at ANL," in *Proc. of Seminar/Workshop on A Review of the Theory and Application of Monte Carlo Methods*, 21-23 April 1980, ORNL-RSIC-44, August 1980.

TABLE 1. Comparison of ZPPR-14 and Typical SP-100 Neutron Balance

SP-100		ZPPR-14
	Production	
1.0000	Fission Source[a]	1.0000
0.0007	(n,2n)	0.0012
	Losses	
0.1052	Capture	0.2329
0.3991	Fission	0.3896
0.3946	Radial Leakage	0.3468
0.1019	Axial Leakage	0.0320

[a]Normalization.

TABLE 2. Analysis of ZPPR-14 Critical Configurations

	ZPPR-14A	ZPPR-14B
Experimental k_{eff}	1.0001 ± 0.0005	1.0004 ± 0.0005
	C/E	
3D Nodal Diffusion[a]	0.9921	0.9796
3D Nodal Transport[a]	0.9964	0.9874
Monte Carlo[b]	0.9962 ± 0.0019	0.9988 ± 0.0020

[a]DIF3D, 30 Groups
[b]VIM

TABLE 3. ^{235}U Fuel Worth in ZPPR-14A

Average Radius (mm)	Worth[a] ($/kg)
39	0.164 ± 0.003
141	0.145 ± 0.002
250	0.100 ± 0.002
305	0.099 ± 0.002

[a] 18.68 kg ^{235}U, 1.10 kg ^{238}U, 1.61 kg stainless steel removed from core. Normalization is to ^{235}U mass.

TABLE 4. Axial Peak/Average Power in ZPPR-14

Radius of Traverse (mm)	ZPPR-14A		ZPPR-14B	
	Peak/Average[a]	C/E[b]	Peak/Average[a]	C/E[b]
13	1.313	0.996	1.634	1.034
69	1.312	0.997	1.627	1.044
124	1.308	1.000	1.656	1.035
179	1.316	0.993	1.682	1.034
234	1.303	1.002	1.751	1.026
290	1.305	1.000	1.880	1.017

[a]From measured $^{235}U(n,f)$ values along axial traverse within ± 839 mm of core midplane.
[b]Ratio of calculation to experiment. (XYZ nodal transport calculation in 30 groups)

TABLE 5. Summary of Core Reaction Rate Ratios in ZPPR-14

Ratio	ZPPR-14A		ZPPR-14B	
	Measured[a]	C/E[b]	Measured[a]	C/E[b]
$^{239}Pu(n,f)/^{235}U(n,f)$	1.102 ± 0.010	0.991 ± 0.008	1.127 ± 0.010	0.997 ± 0.010
$^{238}U(n,\gamma)/^{235}U(n,f)$	0.1241 ± 0.0008	1.033 ± 0.010	0.1218 ± 0.0012	1.015 ± 0.009
$^{238}U(n,f)/^{235}U(n,f)$	0.0412 ± 0.0007	0.992 ± 0.020	0.0455 ± 0.0008	1.018 ± 0.026

[a]Mean value and one standard deviation of 10-20 measurements.
[b]Mean value and one standard deviation of ratios of calculations to experiments (XYZ nodal transport calculation in 30 groups).

TABLE 6. Summary of ZPPR-14 Reflector Worth Results

Reflector Condition	Worth ($)	C/E			
		Nodal Diff.	Nodal Trans.	Monte Carlo	F.D. Diff.[a]
	ZPPR-14A				
1 Segment Removed	6.29 ± 0.12				1.22
3 Segments Removed	20.56 ± 0.39				1.19
4 Segments Removed	29.45 ± 0.62	1.08	1.05	0.969 ± 0.017	1.10
4 Segments Half Withdrawn	9.12 ± 0.17				1.22
4 Void Gaps	6.06 ± 0.11				1.72
	ZPPR-14B[b]				
1 Segment (SS[c])	3.93 ± 0.07				1.40
3 Segments (SS)	11.35 ± 0.32				1.29
4 Segments (SS)	14.42 ± 0.42	1.33	1.17	0.999 ± 0.029	1.22
1 Segment Removed	4.44 ± 0.09				1.33
4 Segments Removed	17.22 ± 0.51	1.20	1.07	0.923 ± 0.030	1.14

[a]Finite difference diffusion calculation in truncated model.
[b]Relative to reference configuration with all 4 segments half withdrawn. (Figure 5)
[c]Secondary Scram configuration, refer to Figure 6.

Figure 1. The ZPPR-14B Assembly with BeO Reflectors in Secondary Scram Configuration

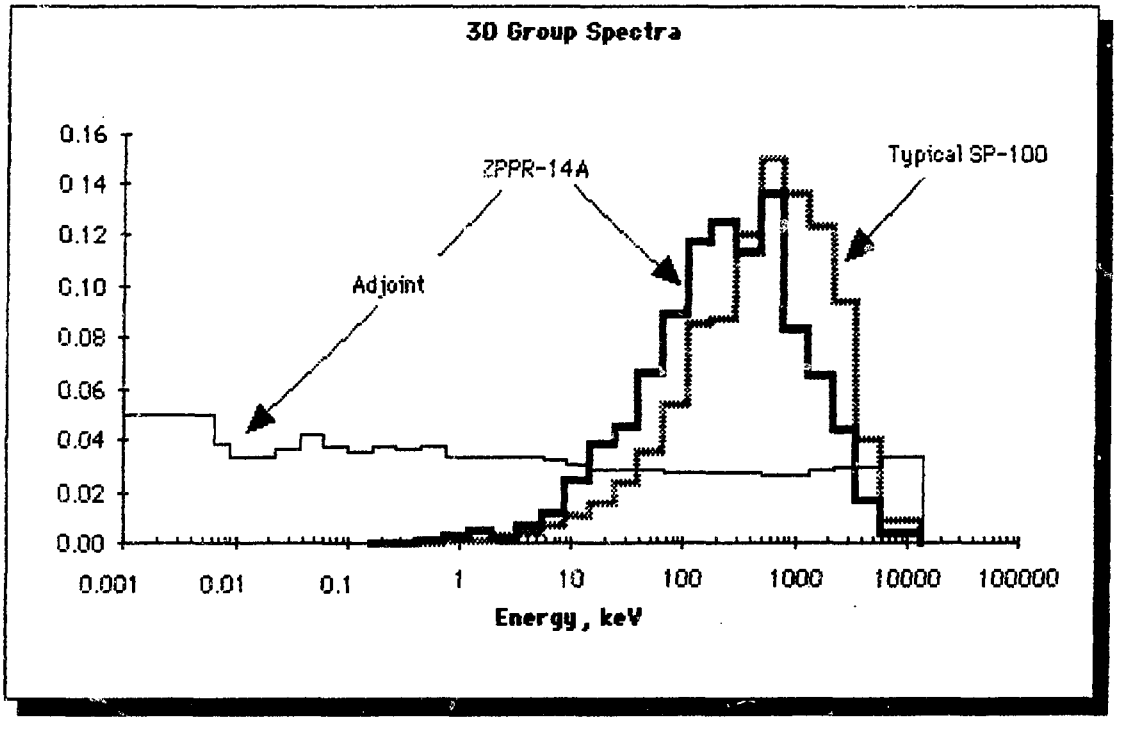

Figure 2. Comparison of ZPPR-14 and SP-100 Neutron Spectra

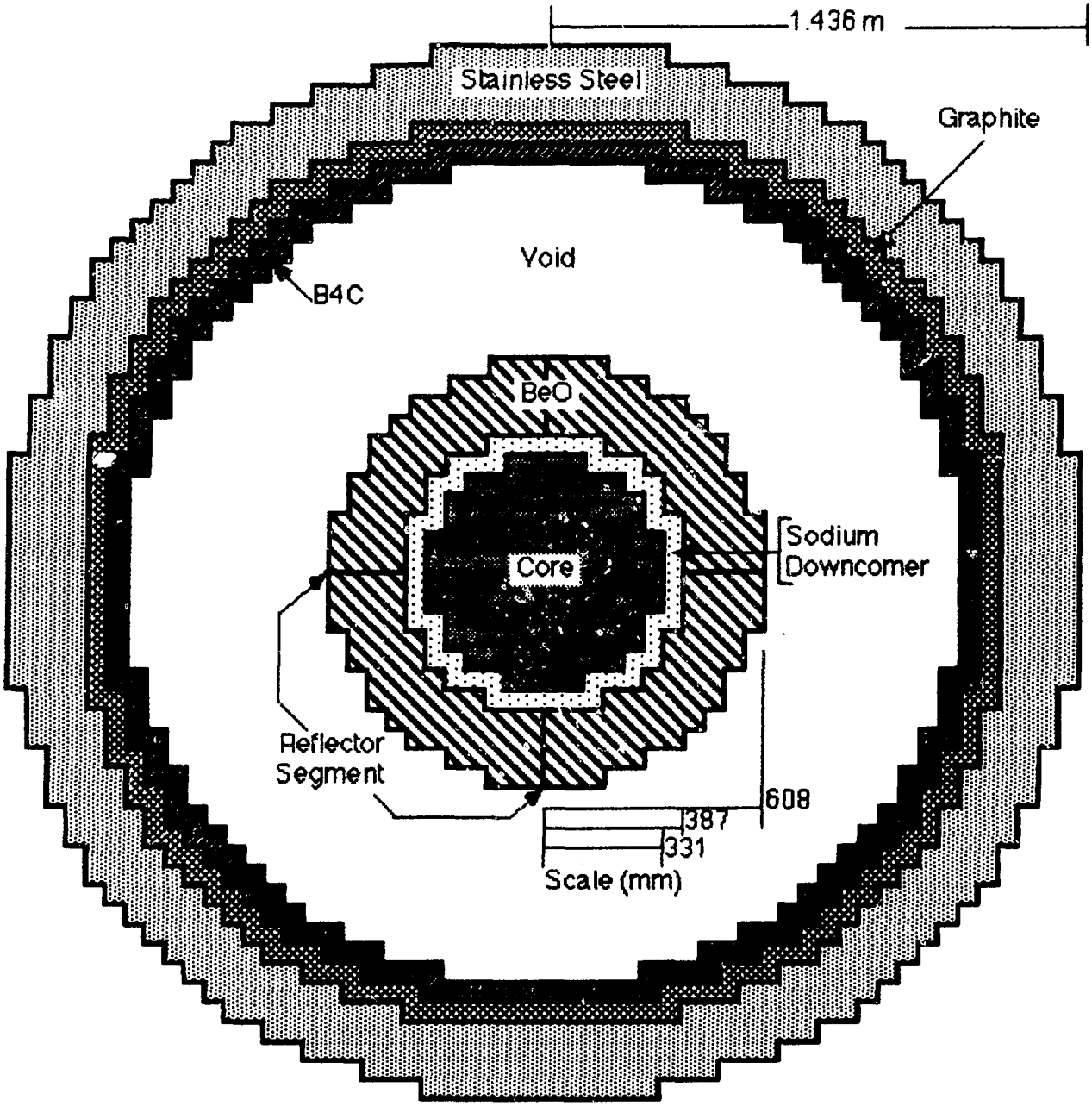

Figure 3. Interface Diagram of ZPPR-14

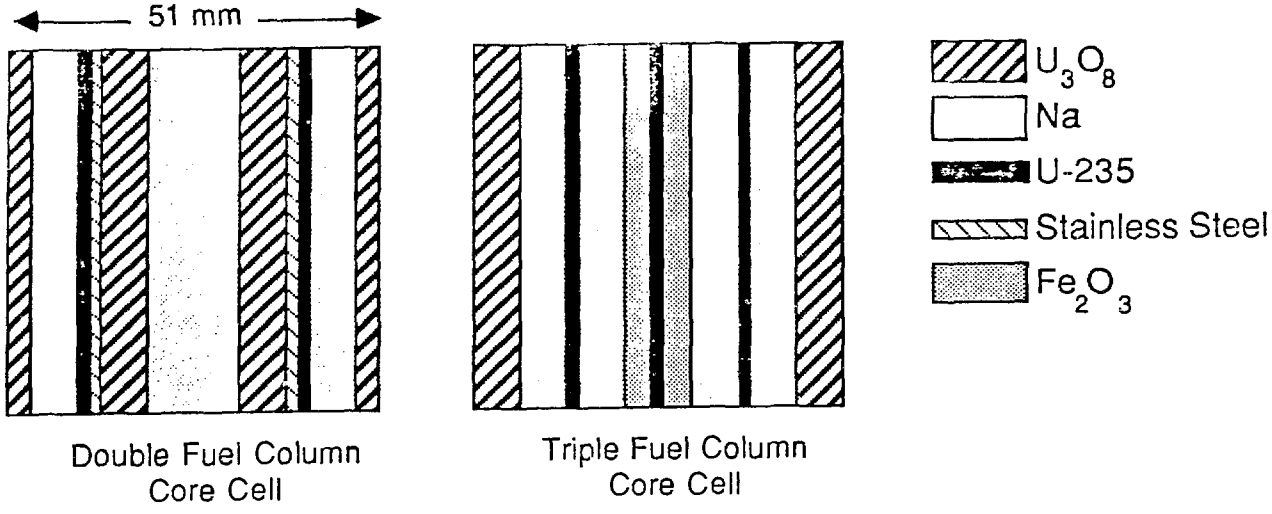

Figure 4. Core Constituents of ZPPR-14

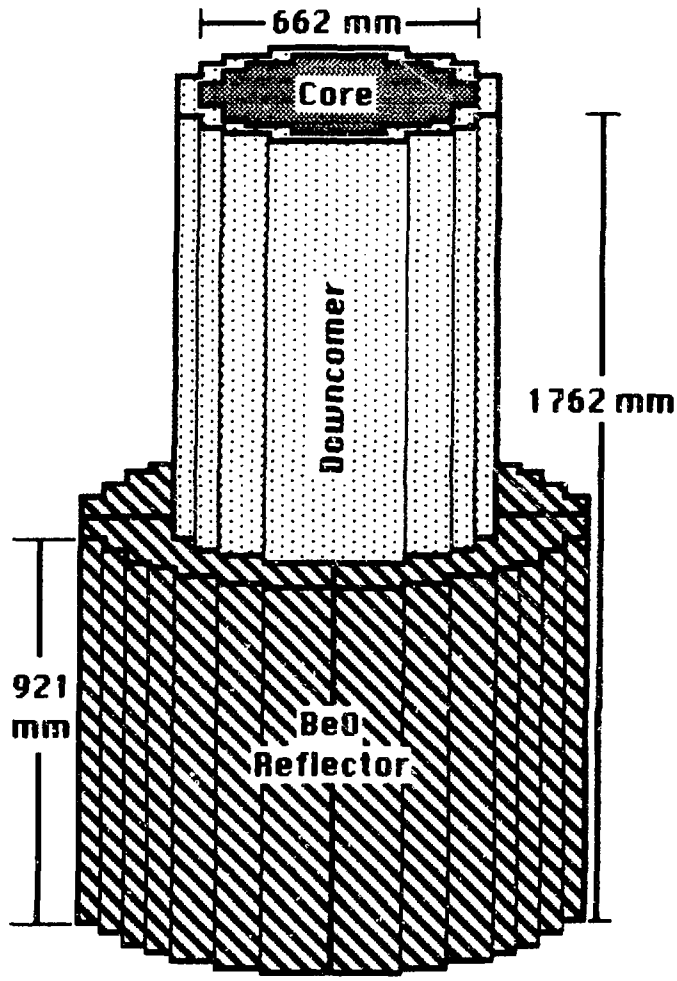

Figure 5. Schematic of the ZPPR-14B Reference Configuration

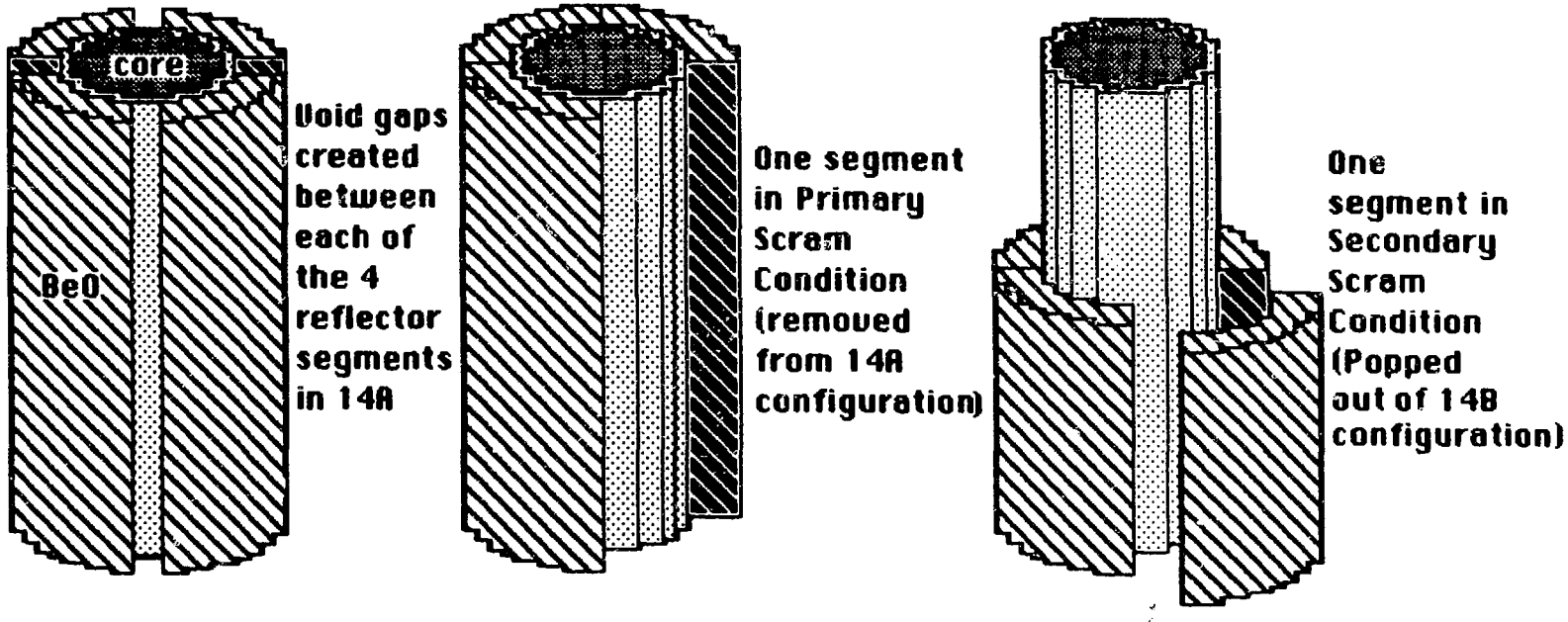

Figure 6. Representative Reflector Perturbations Used in the Worth Measurements

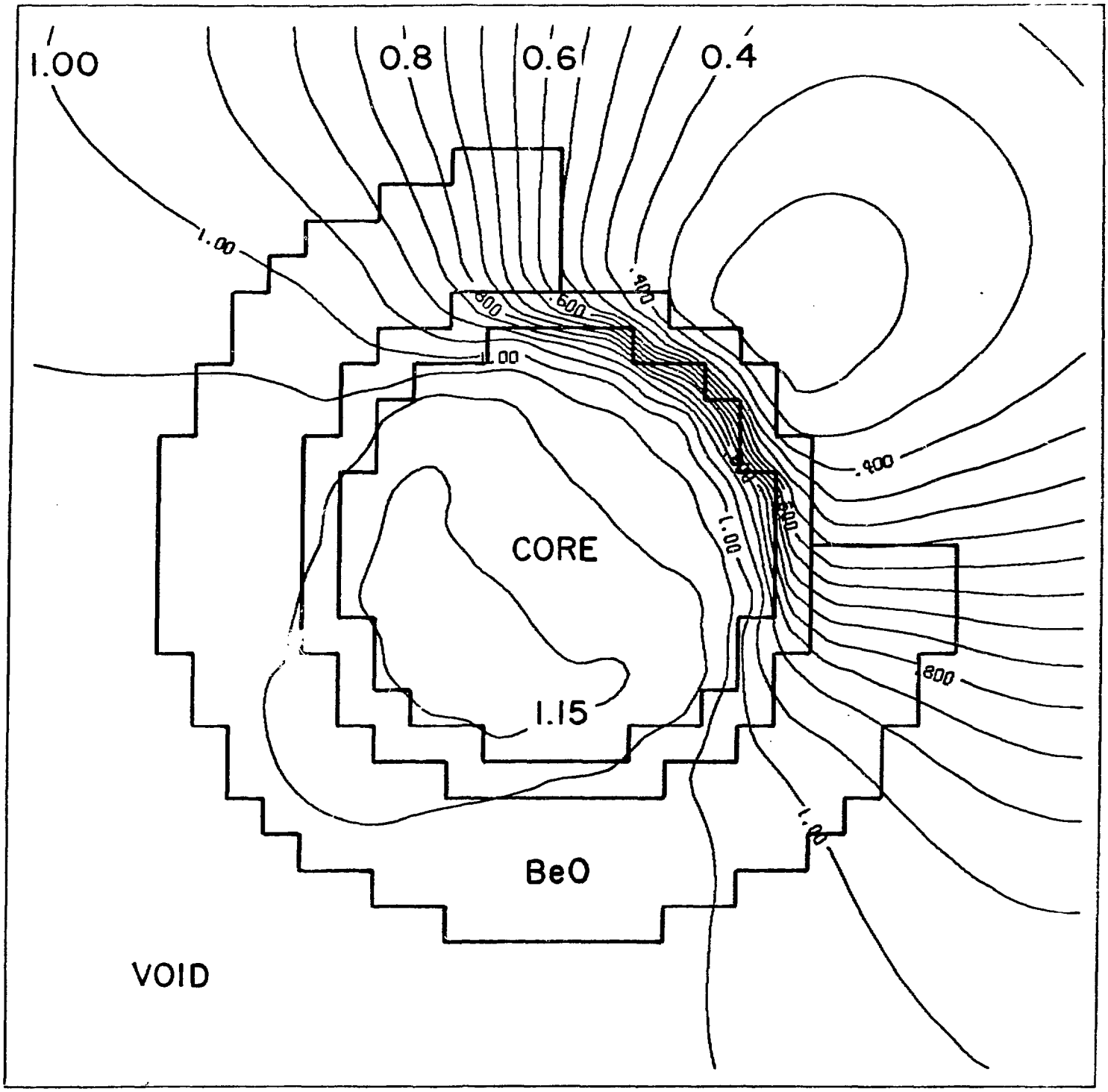

Figure 7. Change in Power Distribution After Removal of Reflector Segment

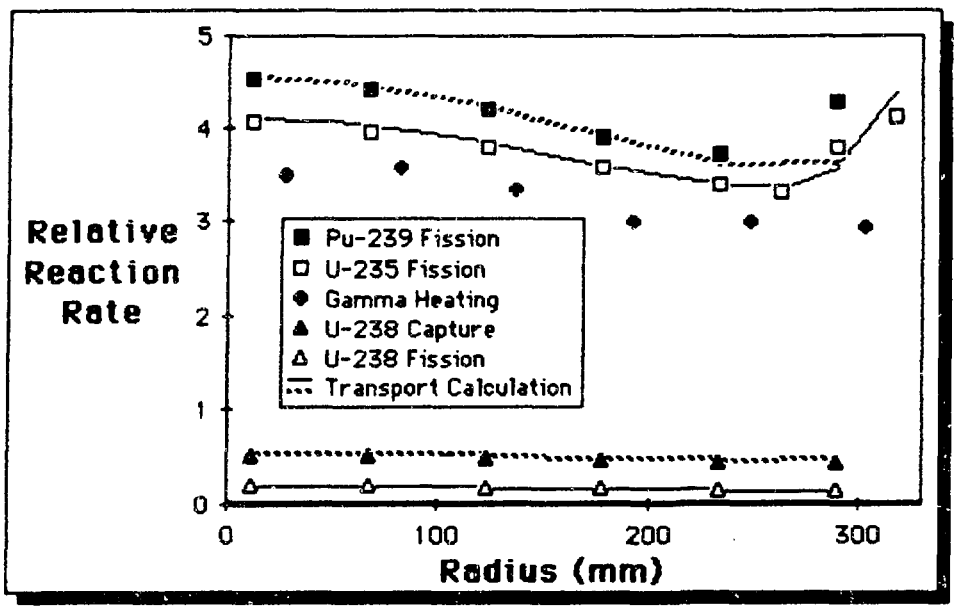

Figure 8. Radial Neutron and Gamma Reaction Rates in ZPPR-14A

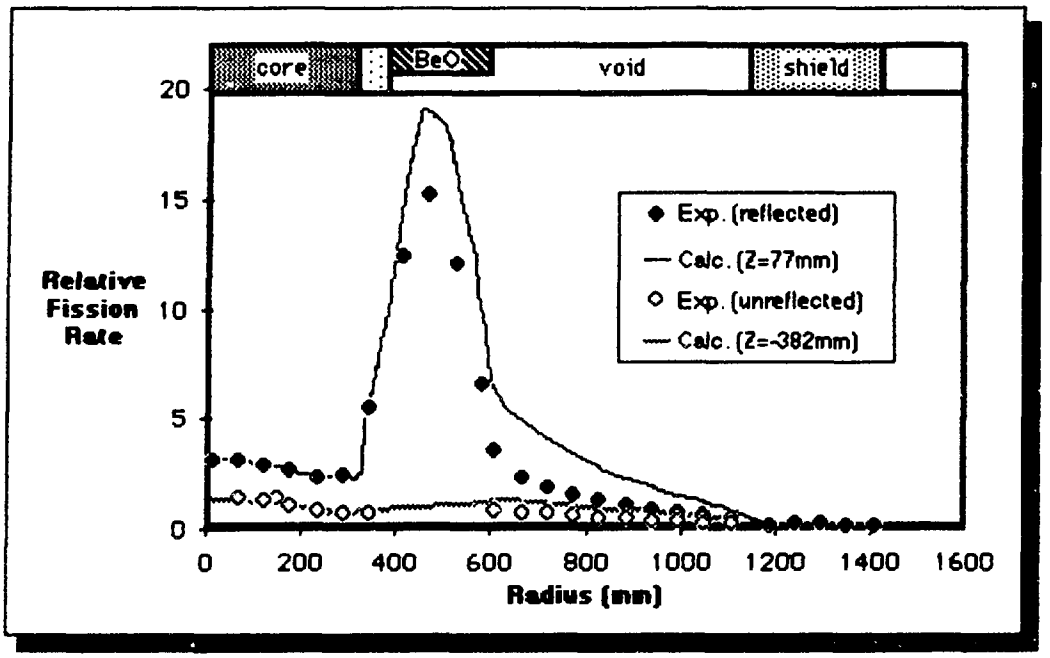

Figure 9. Radial Fission Distribution in ZPPR-14B

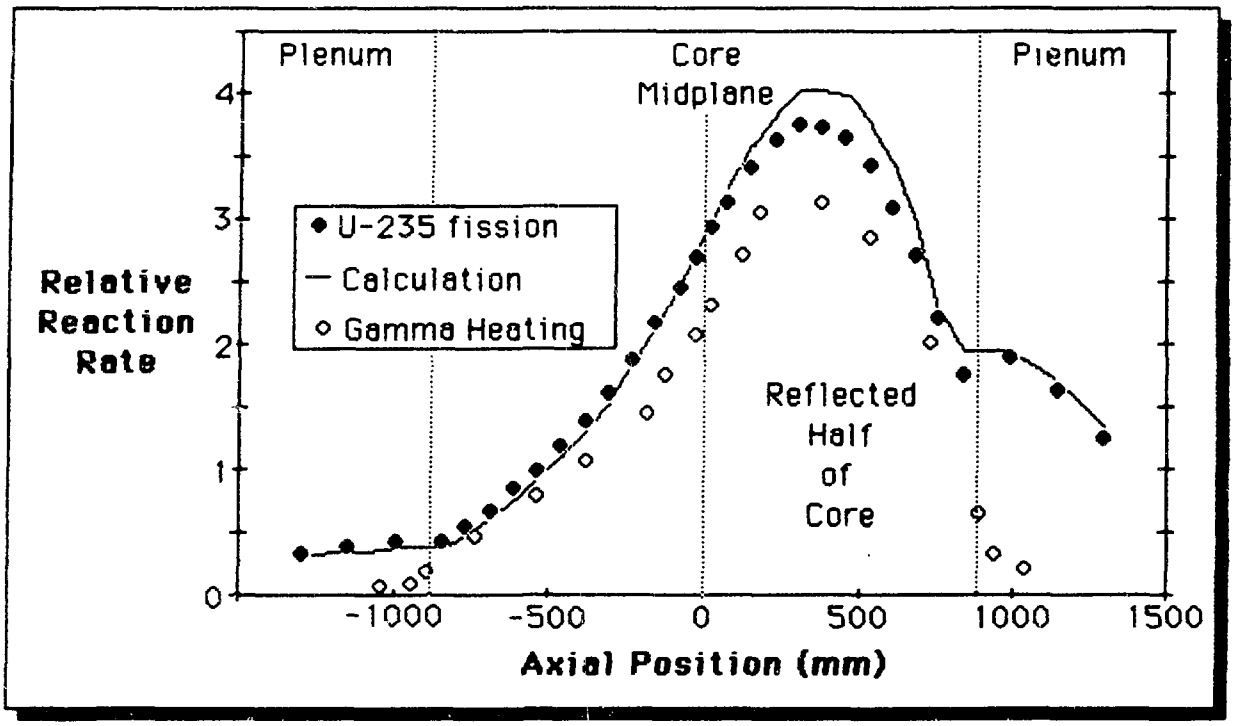

Figure 10. Axial Fission and Gamma Heating Distribution in ZPPR-14B